Neuron, Vol. 31, 593–605, August 30, 2001, Copyright ©2001 by Cell Press

Visualizing Postendocytic Traffic of Synaptic Vesicles at Hippocampal Synapses

Zhiying Li and Venkatesh N. Murthy[1]
Department of Molecular and Cellular Biology
Harvard University
Cambridge, Massachusetts 02138

Summary

We have investigated mechanisms in postendocytic processing of synaptic vesicles at hippocampal synapses, using synaptobrevin/vesicle-associated membrane protein (VAMP) tagged with variants of the green fluorescent protein. Following exocytosis, VAMP is retrieved at synaptic and adjoining axonal regions. Retrieved VAMP-containing vesicles return to synaptic vesicle clusters at a rate slower than endocytosis. Vesicles containing a different protein, synaptophysin, recluster at a similar rate, suggesting common vesicular intermediates for the two proteins. Activity prolongs the time taken by endocytosed vesicles to return to synapses. Exogenous calcium buffers slow endocytosis but have no additional effect on the time course of reclustering. In contrast, the protein kinase inhibitor staurosporine does not affect endocytosis but slows reclustering. Finally, since VAMP can move freely on surface membranes, sustained synaptic activity leads to mixing of this vesicular component between adjacent synapses.

Introduction

The elementary events in vesicular traffic at the presynaptic terminal and their regulation are of fundamental importance to the ongoing communication between neurons (Südhof, 1995; Calakos and Scheller, 1996; Bellen, 1999). Release of neurotransmitter occurs by fusion of synaptic vesicles with the plasma membrane (Katz, 1969; Südhof, 1995; Calakos and Scheller, 1996), and subsequent retrieval of vesicular components by endocytosis ensures restocking of the vesicle pool. Recent investigations have focused on the mode and timing of endocytosis, which remain matters of debate (Koenig and Ikeda, 1989; von Gersdorff and Matthews, 1994; Ryan et al., 1996; Klingauf et al., 1998; Murthy and Stevens, 1998; Brodin et al., 2000; Sankaranarayanan and Ryan, 2001). Clathrin-mediated endocytosis is thought to contribute to membrane and cargo retrieval, and this process is generally imagined to occur at peripheral regions of the synapse away from the active zone (Heuser and Reese, 1973; Miller and Heuser, 1984; Takei et al., 1996; Shupliakov et al., 1997), although this is still debated (Teng and Wilkinson, 2000). A different mode of vesicle recycling is thought to involve transient opening of a fusion pore that allows vesicular contents to be released; rapid closure of this pore leads to recapture of the vesicle, presumably at the active zone itself (Ceccarelli et al., 1973; Fesce et al., 1994; Klingauf et al., 1998; Stevens and Williams, 2000).

Following endocytosis, vesicles are refilled with neurotransmitter and must undergo maturation reactions before becoming release ready. Additionally, they need to be spatially translocated to the releasable pool, which is presumably close to the active zone (Dobrunz and Stevens, 1997; Schikorski and Stevens, 1997). The intervening steps between endocytosis of synaptic vesicles and the next round of exocytosis have remained invisible to conventional electrophysiological methods. In contrast, optical microscopy has provided a window to view some of the steps between endocytosis and subsequent exocytosis of synaptic vesicles (Murthy, 1999; Zenisek et al., 2000).

We have utilized novel fluorescent probes made by attaching variants of the green fluorescent protein to two vesicular proteins, synaptophysin and synaptobrevin/vesicle-associated membrane protein-2 (referred to as VAMP), to visualize different steps in synaptic vesicle trafficking (Miesenbock et al., 1998; Ahmari et al., 2000; Sankaranarayanan and Ryan, 2000). Recently, Ryan and colleagues have used ecliptic synaptopHluorins (ecl-spH), a pH-sensitive version of green fluorescent protein (GFP) fused to VAMP, to trace endocytosis at hippocampal synapses (Sankaranarayanan and Ryan, 2000, 2001). Since ecl-spH becomes essentially invisible once vesicles are endocytosed and acidified, the postendocytic movement of vesicles cannot be easily tracked using this probe. For example, the time course of fluorescence decay in the axonal regions could be due to endocytosis at those locations or movement of plasma membrane resident ecl-spH toward the synaptic region, where endocytosis occurs. In contrast to ecl-spH, attaching EGFP to VAMP might allow the tracking of both endocytosis (since EGFP fluorescence is also pH sensitive) and subsequent transport (since EGFP will still be visible at vesicular pH). It is also of interest to determine the postendocytic fate of other vesicular proteins such as synaptophysin. In this study, we make use of these probes to visualize three different steps in the synaptic vesicle cycle: exocytosis, endocytosis, and subsequent transport of vesicles.

As reported recently (Sankaranarayanan and Ryan, 2001), most of the action potential-evoked exocytosis involves complete fusion of synaptic vesicles with and insertion of VAMP into the plasma membrane. We find that subsequent retrieval of VAMP occurs all along the axonal regions adjacent to the release sites. Retrieved vesicular components are efficiently transported to vesicular clusters in the central regions of the synapse. Endocytosis and transport are slowed down by activity. Buffering intracellular calcium slows endocytosis as reported recently (Sankaranarayanan and Ryan, 2001) but has no additional effect on reclustering time course. Reclustering is not affected by disruption of actin filaments or microtubules but is sensitive to perturbation of protein kinases. Importantly, because there is no clear barrier for movement of VAMP along the axonal surface, recycling results in the exchange of vesicular compo-

[1] Correspondence: vnmurthy@fas.harvard.edu

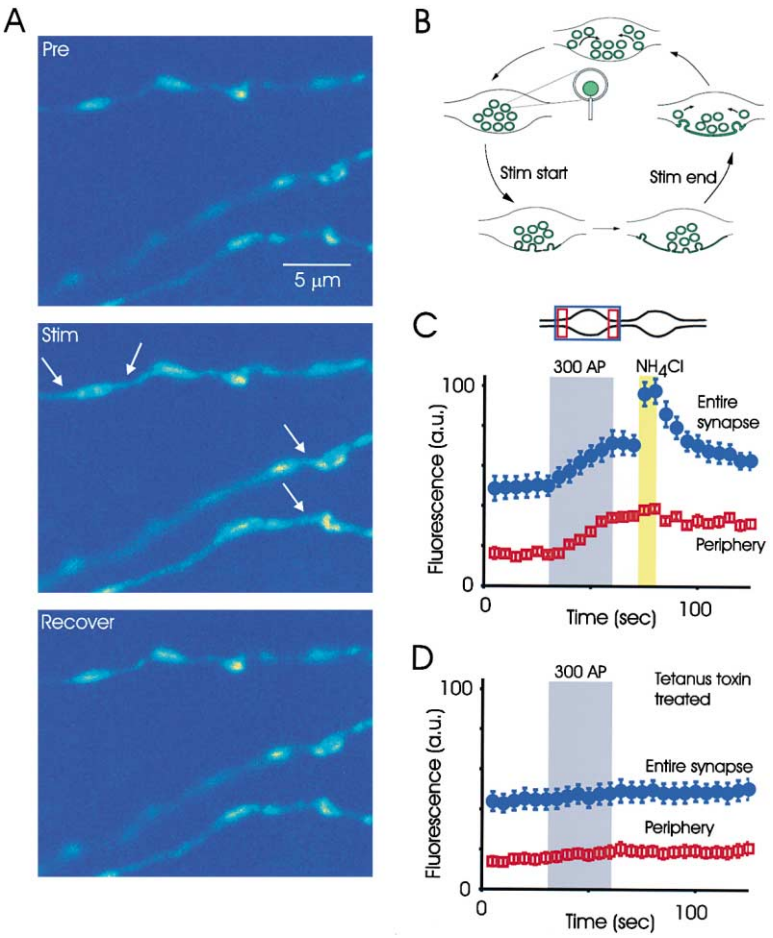

Figure 1. Activity-Dependent Dispersion of VAMP-EGFP at Synapses

(A) Fluorescence image of a set of synapses expressing VAMP-EGFP. Delivering 300 action potentials at 10 Hz causes synapses expressing VAMP-EGFP to become elongated and the axonal regions to become brighter (arrows). After stimulation is terminated, synapses recover their prestimulus fluorescence distribution.

(B) Model used to interpret the fluorescence spread and recovery. Under resting conditions, fluorescence is clustered within the synapse. Upon stimulating, VAMP-EGFP is inserted into the plasma membrane and diffuses to the periphery. Endocytosis occurs in the peripheral regions (as well as the central regions). The endocytosed VAMP-EGFP is then transported back to the vesicle cluster. Green regions of the membrane denote VAMP-EGFP.

(C) Alkalinization of synapses using NH_4Cl reveals that most of VAMP-EGFP in the peripheral regions is on the surface soon after stimulation. The fluorescence intensity over the entire synapse (red circles) increases during a 300 AP stimulus as expected from the pH sensitivity of EGFP (see Appendix). About 10 s after termination of stimulus, the acidic pH in synaptic vesicles was neutralized using NH_4Cl (yellow stripe). While the fluorescence intensity in the synaptic regions increases (circles), intensity in the peripheral/axonal regions does not increase substantially (squares). The slow decay after cessation of NH_4Cl stimulus is presumably due to slower exchange of fresh medium.

(D) Treatment with tetanus toxin, which cleaves VAMP/synaptobrevin, prevents activity-dependent dispersion of VAMP-EGFP. The ordinate has been chosen to match that in (C) for easy visual comparison.

nents between neighboring synapses during periods of intense activity.

Results

Activity-Dependent Dispersion of VAMP-EGFP

We first confirmed previous reports (Miesenbock et al., 1998; Ahmari et al., 2000; Sankaranarayanan and Ryan, 2000) indicating that VAMP-EGFP and synaptopHluorins are targeted to synapses and do not appear to compromise presynaptic function (see supplemental data at http://www.neuron.org/cgi/content/full/31/4/593/DC1). If VAMP-EGFP is resident on synaptic vesicles, it will be recycled in an activity-dependent manner along with the synaptic vesicle membrane. In particular, recycling might entail insertion into the plasma membrane and subsequent movement to the edges of the synapse where endocytosis is thought to occur. To look for such movement of VAMP-EGFP, we imaged synapses before, during, and after exocytosis triggered by action potentials. When a stimulus of 300 action potentials is delivered, fluorescence spots became elongated along the axis of the axon (Figure 1A). Remarkably, when electrical stimulation was terminated, the distribution of fluorescence recovered to a clustered form (Figure 1A).

We interpret this spread of fluorescence along the axon and subsequent reclustering in terms of the following model (Figure 1B). At rest, most of the fluorescence is associated with synaptic vesicles, which are present in a tight cluster. Upon stimulation, VAMP-EGFP is incorporated into and spreads along the presynaptic plasma membrane onto adjacent axonal regions. Endocytosis occurs in the peripheral regions (and perhaps also in the central region), and the endocytosed vesicles recluster in the central region of the bouton. We present evidence below for each of the steps in the proposed model.

VAMP-EGFP Diffuses in the Plasma Membrane following Exocytosis

The first question that arises is whether the dispersion of fluorescence to the intersynaptic axonal regions upon stimulation reflects diffusion of VAMP on the surface membrane or intracellular movement of vesicles. Several observations suggest that the fluorescence dispersion we observe is dependent on exocytosis and subsequent diffusion of VAMP-EGFP in the plasma membrane. First, when FM1-43-labeled synapses are stimulated, one does not observe any lateral movement of fluorescence; there is only the slow loss of fluorescence at

synaptic sites due to exocytosis. Second, the same dispersion is observed with ecl-spH (Sankaranarayanan and Ryan, 2000; our data). Since ecl-spH is nearly invisible when resident on vesicles, the visible dispersion could only reflect movement of plasma membrane-resident proteins.

A third argument supporting dispersion of VAMP along the plasma membrane comes from the following experiment suggested by a recent study using ecl-spH (Sankaranarayanan and Ryan, 2001). We used the pH dependence of EGFP fluorescence to measure the time course of exocytosis and endocytosis. EGFP fluorescence increases 3-fold when going from the acidic environment within vesicles (pH $\sim$5.5) to the neutral environment of the extracellular space (Kneen et al., 1998; Llopis et al., 1998; Han et al., 1999) (our unpublished data). If the increase in fluorescence intensity in the perisynaptic regions is due to intracellular movement of intact vesicles, then neutralizing the vesicular pH using NH_4Cl should lead to an increase in the fluorescence intensity in the axonal regions. In contrast, if the rise in fluorescence intensity in the perisynaptic regions following stimulation is due to surface diffusion of VAMP, adding NH_4Cl should not lead to significant addition of fluorescence (since there are no intracellular vesicles in the axonal regions). We found less than 15% increase in the axonal fluorescence upon addition of NH_4Cl (Figure 1C). This argues strongly that the fluorescence increase in the axonal regions is due to movement of VAMP incorporated into the plasma membrane.

Finally, we ruled out activity-dependent lateral dispersion of intracellular vesicle cluster by using tetanus toxin to inhibit exocytosis without altering calcium influx (Schiavo et al., 1992). After incubating cultures in tetanus toxin for 16 hr, evoked release is severely impaired (Neale et al., 1999; Figure 1D, no change in fluorescence over the synapse). This toxin does not affect action potential-evoked calcium influx into synaptic terminals (Dreyer et al., 1983). If calcium-mediated signaling were to free vesicles from their cluster and disperse them laterally, we would observe this as an increase in the fluorescence in the peripheral regions of the synapse. This was not the case in three of three experiments (Figure 1D), strengthening the argument that dispersion of VAMP-EGFP into intersynaptic axonal regions is due to exocytosis and subsequent diffusion on the plasma membrane.

Reclustering Is Separable from Endocytosis

Recently, ecl-spH has been used to track endocytosis at hippocampal synapses (Sankaranarayanan and Ryan, 2000, 2001). Since this probe is hardly fluorescent once internalized, movement of vesicles following endocytosis could not be visualized in those experiments. VAMP-EGFP, because of its smaller fluorescence change between vesicular and neutral pH, is still visible at acidic pH of vesicles. We reasoned that this would permit visualization of additional steps beyond endocytosis. Following exocytosis, there will be two pools of VAMP-EGFP in the peripheral regions: exposed and internalized VAMP-EGFP. There are two processes that cause reduction of the fluorescence in the periphery: endocytosis (and immediate acidification) and movement of internalized VAMP-EGFP to the center of the synapse. If each of these processes is considered to occur nearly irreversibly on the time scale and conditions of our experiments, a simple analytical solution can be obtained in terms of the rate constants for the two processes (see Appendix). By measuring the fluorescence change over the entire synapse—the central region of the bouton and the adjacent axonal regions—we obtain the time course of endocytosis. Reclustering time course is estimated by measuring fluorescence change in the perisynaptic regions (Figure 2A).

The results from a single experiment using VAMP-EGFP are illustrated in Figure 2B. The experiments confirm our prediction that peripheral fluorescence should recover more slowly than the overall fluorescence at the synapse. Therefore, we were able to measure the time course of movement of vesicles from the perisynaptic regions to the synaptic cluster. After a stimulus of 300 action potentials, fluorescence reclustering occurred with a time constant of 118.2 $\pm$ 8.95 s (n = 302 synapses, 15 experiments). In comparison, the time constant of endocytosis estimated using VAMP-EGFP is 67.3 $\pm$ 6.55 (n = 302 synapses, 15 experiments).

The reclustering observed in these experiments could reflect transport of plasma membrane-resident VAMP-EGFP, or vesicle-resident VAMP-EGFP. If VAMP-EGFP remained on the plasma membrane as it moved from the peripheral regions back to the central regions, the time course of reclustering would essentially reflect the time course of endocytosis. As shown in Figure 2B, this is not so for VAMP-EGFP. To further illustrate this point, we compared the time course of fluorescence loss in the peripheral regions with that for the entire synapse in experiments using ecl-spH. Since acidification of synaptic vesicles occurs rapidly upon endocytosis (Sankaranarayanan and Ryan, 2000), the fluorescence change of ecl-spH would reflect endocytosis, whether measured in the peripheral regions or over the entire synapse.

Figure 2C shows a typical experiment with a set of synapses expressing ecl-spH. The time course of recovery of fluorescence at peripheral regions was indistinguishable from the time course for the entire synapse (entire synapse: 66.1 $\pm$ 6.58 s, periphery: 68.6 $\pm$ 8.23, n = 240 synapses, ten experiments). This is in contrast to the behavior of VAMP-EGFP (Figure 2B). Therefore, we conclude that the slower fluorescence recovery seen at the periphery with VAMP-EGFP reflects the transport of vesicles back to the center. Our experiments do not rule out simultaneous endocytosis in the central regions. Since the time course of recovery of fluorescence is similar in the central and the peripheral regions for ecl-spH, it seems reasonable to assume that endocytosis proceeds at a similar rate in both regions.

Synaptophysin-EGFP Dispersion and Reclustering Are Similar to Those of VAMP-EGFP

To determine if other vesicular components exhibit similar rates of reclustering, we examined the movement of synaptophysin-EGFP following action potential stimulation. If, as suggested in recent years (Takei et al., 1996; Murthy and Stevens, 1998), endocytosis at synapses results in efficient capture of vesicular components with-

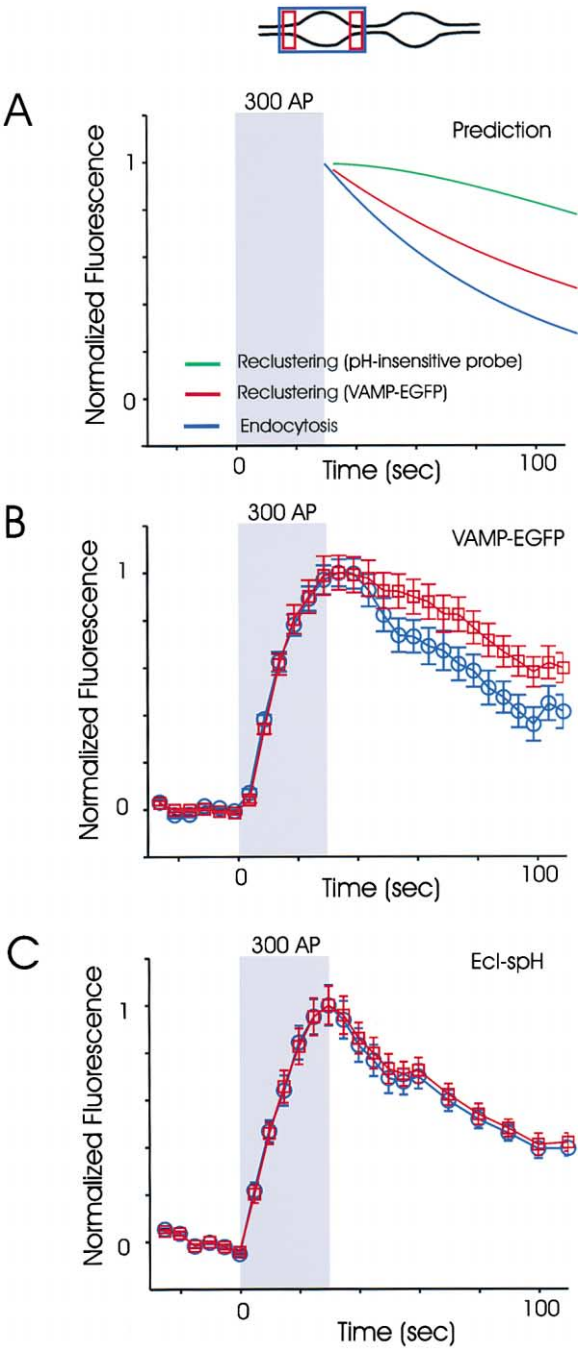

Figure 2. Separating Transport of VAMP-EGFP Vesicles from Endocytosis

(A) Theoretical prediction of the time course of fluorescence measured over the entire synapse (blue circles) or just the peripheral regions (red squares). The graph shows the time course of recovery in the peripheral regions for a probe with no pH dependence (green) and for VAMP-EGFP, which has some pH dependence (red). The fluorescence intensity measured over the entire synapse reflects only endocytosis (blue); this is what ecl-spH is expected to report, whether measured at the periphery or over the entire synapse.

(B) Fluorescence recovery over the entire synapse as well as just the peripheral regions, measured using VAMP-EGFP. Note that the time course in the peripheral regions is significantly slower than the time course over the whole synapse. The stimulus was 300 action potentials at 10 Hz, indicated by the gray bar. Data obtained from a single experiment (ten synapses).

(C) A similar experiment performed using ecl-spH fails to reveal a difference in the time course, suggesting that endocytosis occurs at equal rates in the peripheral and central regions (single experiment, ten synapses).

out the need for further sorting, postendocytic movement of different vesicular components would occur at similar rates. Synaptophysin-EGFP was targeted to synapses and did not alter presynaptic function (Figures 3A–3C). In response to 300 APs at 10 Hz, dispersion and reclustering of synaptophysin-EGFP were also essentially identical to those of VAMP-EGFP (Figure 3D). Since EGFP is cytoplasmic in this fusion protein, exocytosis did not lead to a significant increase in the fluorescence of this reporter. The dispersion of the protein to axonal regions, however, mimicked VAMP-EGFP dispersion. After termination of stimulation, recovery of fluorescence in the axonal region occurred after a short delay, at a rate very similar to VAMP-EGFP (time constant of 115.4 $\pm$ 6.81 s, n = 46 synapses, three experiments; Figure 3D).

Time Course of Reclustering Is Slowed by Activity but Is Unaffected by Exogenous Calcium Buffers

Since the time course of endocytosis is altered by activity (Sankaranarayanan and Ryan, 2000), we wondered if reclustering was also affected by activity. We used VAMP-EGFP-expressing neurons to measure reclustering rates as a function of stimulus duration. In addition, we used ecl-spH to measure rates of endocytosis because of its better signal-to-noise ratio. Figure 4A shows the average time course of endocytosis following 100 AP and 300 AP stimulus from one experiment. The time constant following 300 AP is clearly larger than that for 100 AP, and this was confirmed by averages from multiple experiments. Figure 4B shows that the time course of reclustering is also significantly altered by the amount of exocytosis evoked. In fact, as seen in Figure 4C, the time course of reclustering was slower than the time course of endocytosis for each stimulus strength. This suggests that at least two separate steps in the recycling process are altered by activity. We tested whether the variation in the time course of recovery observed in different experiments in which identical stimuli were delivered was due to variation in the degree of exocytosis. As seen in Figure 4D, there was a strong correlation between the fractional fluorescence change (related to exocytosis) and the time constant of endocytosis as well as reclustering ($r^2 > 0.9$, $p < 0.01$ for both quantities). This suggests that, even for a constant stimulus, the actual degree of exocytosis determines the subsequent rate of endocytosis and reclustering.

There is increasing evidence for the requirement of calcium ions in endocytosis at synapses (Gad et al., 1998; Neale et al., 1999), and recent studies have indicated that calcium might accelerate endocytosis at hippocampal synapses (Klingauf et al., 1998; Sankaranarayanan and Ryan, 2001). A logical next step was to determine if signaling by calcium was involved in reclustering. We used EGTA-AM to introduce exogenous cal-

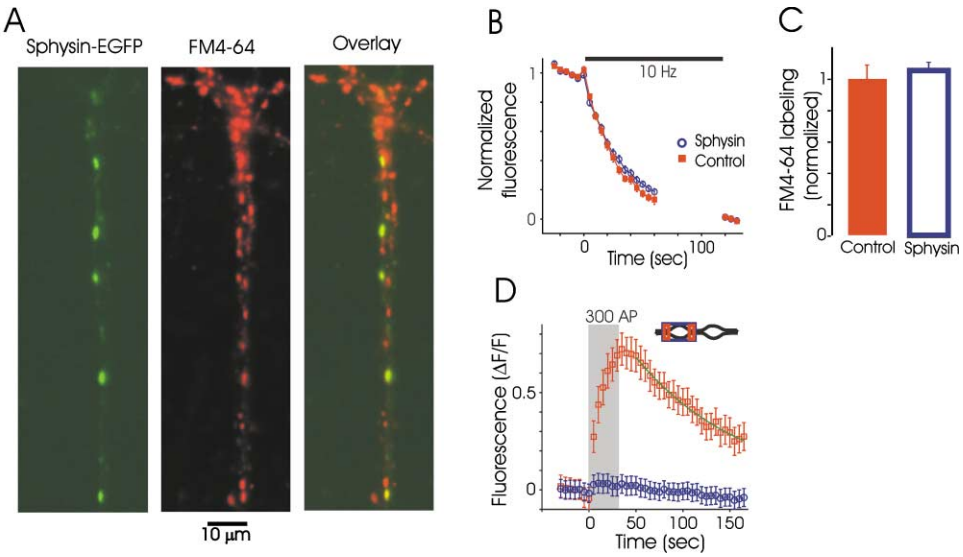

Figure 3. Dynamics of Synaptophysin-EGFP

(A) Simultaneous fluorescence imaging shows colocalization of synaptophysin-EGFP and FM4-64. The many FM4-64 puncta without corresponding synaptophysin-EGFP spots are synapses made by axons not expressing synaptophysin-EGFP, which vastly outnumber transfected axons.

(B) The fractional rate of exocytosis, measured using FM4-64 destaining, is not significantly different at synapses expressing synaptophysin-EGFP, when compared to control synapses. The slightly slower destaining at longer times did not reach statistical significance ($p > 0.1$, $n = 31$ synapses, from two experiments).

(C) The average amount of FM4-64 labeling in response to a 300 action potential stimulus at 10 Hz was not significantly different between synaptophysin-EGFP-expressing and control synapses ($p > 0.1$, $n = 31$, from two experiments). This indicates that neither release nor endocytosis is significantly affected by expression of synaptophysin-EGFP. Data are normalized to the average fluorescence intensity of control synapses.

(D) Activity-dependent dispersion and recovery of synaptophysin-EGFP at a set of synapses. Fluorescence in the intersynaptic regions (red squares) increases upon stimulation (300 APs at 10 Hz) and then recovers to resting levels after termination of stimulus. Total fluorescence over the entire synapse does not change significantly (blue circles). The kinetics of recovery of fluorescence in the peripheral regions could be fitted well with a single exponential function, beyond an initial delay (note the first four points after stimulus offset). The average rate of decay was 115.4 ± 6.8 s ($n = 46$ synapses, three experiments). Inset shows a schematic drawing of synaptic boutons, and the boxes represent regions over which intensities were measured.

cium buffers into neurons and measured the time course of endocytosis and reclustering. EGTA reduces the maximal change in fluorescence upon stimulation, indicating a reduction in exocytosis. This is not surprising, since EGTA is expected to decrease facilitation and asynchronous release at these synapses (Cummings et al., 1996). Additionally, we find that the time course of endocytosis is slowed by EGTA (Figure 5). The time course of reclustering is not altered significantly when release is evoked by 300 action potentials (Figure 5). For the 100 action potential stimulus, reclustering time is slightly increased, but this increase simply reflects the lengthening of the period of endocytosis; this is expected, since reclustering occurs only following endocytosis. Figure 5C summarizes the data for experiments in which the same set of synapses were studied before and after addition of EGTA-AM. The ratio of the time constant after EGTA-AM treatment to the time constant before treatment reveals a significant slowing of endocytosis ($p < 0.01$, paired t test) and no change in reclustering time course ($p > 0.4$).

What Are the Mechanisms in Reclustering?

Since endocytosed synaptic vesicles return to the synapse rather than assuming a uniform distribution in the axon, we suspected an active mechanism in the transport of these newly endocytosed vesicles. We first tested the role of cytoskeletal elements actin and microtubules, since isoforms of myosin and kinesin are thought to be associated with synaptic vesicles (Prekeris and Terrian, 1997; Yonekawa et al., 1998). We treated cells with 20 μM latrunculin A, which causes depolymerization of actin in many cells, and 10 μM nocodazole, which destabilizes microtubules. These agents did not have a significant effect on the time course of endocytosis or reclustering (Figure 6A). We confirmed that latrunculin A was active by the severe changes in the morphology of cultures and the loss of actin in EGFP-actin-expressing dendritic spines (data not shown). Nocodazole activity was confirmed by the reduction in movement of vesicles in the axonal regions. Our results are nevertheless somewhat inconclusive, since we were unable to confirm directly that a dynamic cytoskeleton is absent at the presynaptic terminal because of the small size of the terminals.

We next investigated the role of protein kinases in reclustering using the nonspecific kinase inhibitor staurosporine. This compound is thought to inhibit protein kinase C, as well as other kinases, such as calcium/calmodulin-dependent kinases. Staurosporine decreases the amount of exocytosis, as evidenced by a decrease in the amount of fluorescence (Table 1). This effect can

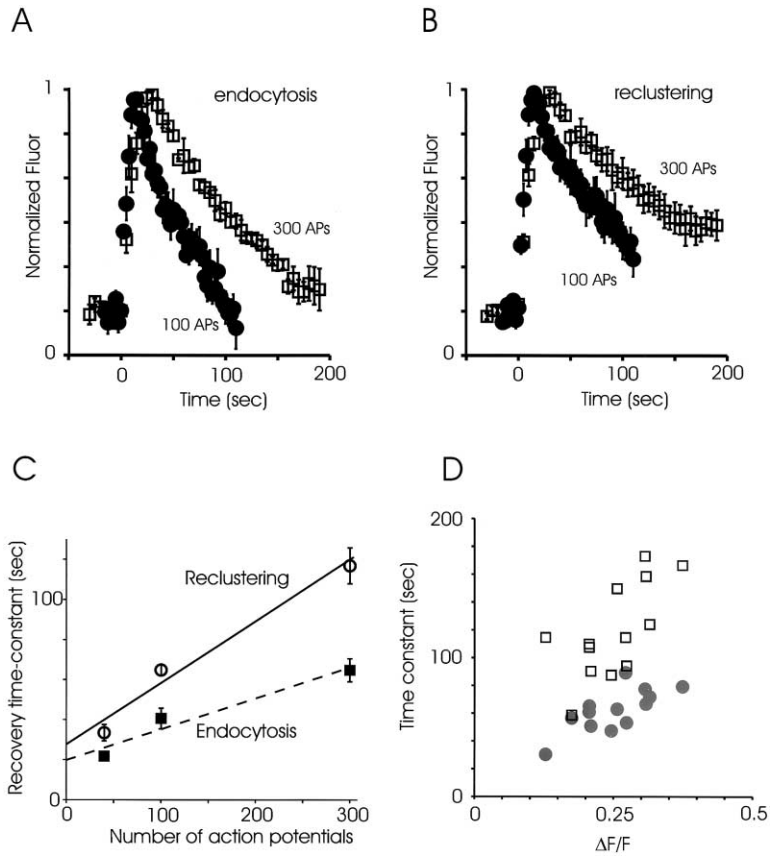

Figure 4. The Time Course of Endocytosis and Reclustering Depends on the Strength of Stimulus

(A and B) Average time course of endocytosis measured using VAMP-EGFP for two different stimulus durations: 100 and 300 action potentials at 10 Hz (solid circles and hollow squares, respectively). With increasing activity, both endocytosis and reclustering are prolonged.

(C) Dependence of rates of endocytosis and reclustering on number of action potentials. Each point represents at least five experiments and greater than 50 synapses. Endocytosis time constants for 40, 100, and 300 AP stimuli were, respectively, 21.8 ± 1.43, 40.6 ± 5.20, and 64.7 ± 5.77 s. Reclustering time constants for 40, 100, and 300 AP stimuli were, respectively, 33.4 ± 4.13, 64.8 ± 2.54, and 116.8 ± 8.92 s. The lines are best-fitting linear regressions.

(D) The time constant of endocytosis (solid circles) and reclustering (squares) plotted against the fractional change in fluorescence for 13 experiments in which 300 action potentials were delivered. There is a strong correlation ($r^2 > 0.9$ for endocytosis and reclustering, $p < 0.01$) between the amount of exocytosis and the rates of endocytosis and reclustering.

be due to an impairment of the mobilization of synaptic vesicles (Becherer et al., 2001) or a speeding up of endocytosis (Klingauf et al., 1998). We do not find evidence for speeding of endocytosis, at least after cessation of the stimulus (Table 1, Figure 6B). The most robust effect was a nearly 2-fold slowing of reclustering (Table 1, Figure 6B).

Protein kinase C (PKC) has been implicated in vesicle mobilization in some synapses (Stevens and Sullivan, 1998). Since PKC is one of the targets of staurosporine, we wondered whether activation of PKC has an effect on reclustering. We treated neurons with the phorbol ester phorbol 12-myristate 13-acetate (PMA) for 10 min and investigated its effect on the extent and time course of exocytosis, endocytosis, and reclustering. Previous studies indicate that phorbol esters increase spontaneous as well evoked release during low-frequency stimulation (Parfitt and Madison, 1993; Stevens and Sullivan, 1998; Waters and Smith, 2000). Our experiments indicate that during higher frequency stimulation (10 Hz), release during the first few stimuli is increased in PMA-treated synapses compared to those treated with the inactive phorbol ester, 4α-phorbol 12-myristate 13-acetate (fractional fluorescence increase after 50 APs was 0.061 ± 0.013 in control synapses and 0.116 ± 0.021 in PMA-treated synapses, n = 4 experiments). The fluorescence increase after 300 stimuli, however, is not significantly different from control (Table 1). The time course of endocytosis and reclustering were also not significantly different (Table 1, Figure 6C).

Dispersion of VAMP Leads to Mixing between Adjacent Synapses

Our findings suggest that, following exocytosis, vesicular VAMP can diffuse along the axonal membrane adjacent to synaptic boutons. We wondered if this dispersion could lead to mixing of synaptic vesicle proteins between neighboring synapses. To test this, we used the method of fluorescence recovery after photobleaching. Using high-intensity laser illumination, we first photobleached a VAMP-EGFP-labeled synapse. If there were no movement of vesicles between synapses, the photobleached synapse should not recover much fluorescence as long as the synapse is at rest (some recovery is expected, since there will be exchange of surface VAMP with neighboring axonal regions). This was indeed the case for periods of minutes (Figure 7). In contrast, when synaptic activity is evoked, unbleached VAMP-EGFP from neighboring synapses will diffuse along the axon and will be incorporated into newly formed vesicles of the bleached synapse. This prediction is confirmed by experiments (Figure 7).

Several arguments support the idea that the recovery of fluorescence in bleached synapses is due to movement of VAMP-EGFP from neighboring synapses. First, the total fluorescence measured over several synapses shows an increase upon stimulation (due to pH change encountered by VAMP-EGFP) but recovers to its prestimulus value after stimulus is terminated (Figure 7, line labeled "1+2+3"). The fluorescence in the bleached synapse, however, shows a net increase after stimulation

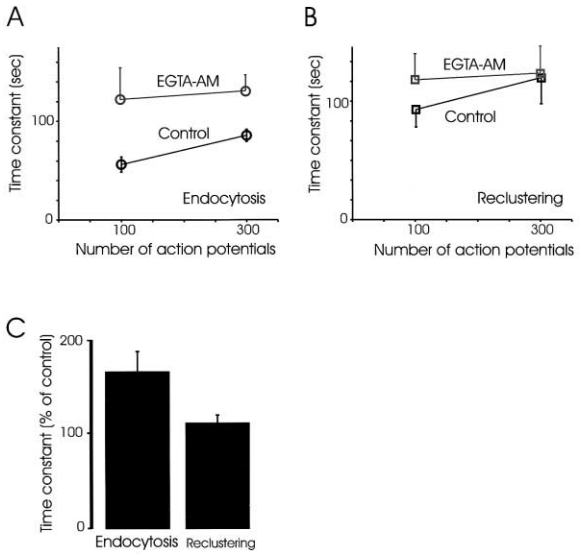

Figure 5. Endocytosis but Not Reclustering Is Prolonged by Exogenous Calcium Buffers

(A and B) The time constant of endocytosis and reclustering for two stimulus strengths for control synapses and for synapses treated with EGTA-AM. Endocytosis is slower after treatment with EGTA-AM for both stimulus strengths ($p < 0.01$, t test), while reclustering is not significantly altered ($p > 0.1$). Endocytosis time constants for 100 and 300 AP stimuli were, respectively, 56.3 ± 7.7 s and 81.6 ± 6.1 s (control), 122.0 ± 36.9 s and 130.8 ± 15.2 s (EGTA-AM). Reclustering time constants for 100 and 300 AP stimuli were, respectively, 111.5 ± 17.7 s and 143.4 ± 26.1 s (control), 141.7 ± 30.4 s and 144.5 ± 28.6 s (EGTA-AM). Data are from at least four experiments and 50 synapses for each condition.

(C) For experiments in which measurements were made both before and after treatment with EGTA-AM, paired comparisons could be made. The time constant of endocytosis after EGTA-AM treatment was increased to ~164% of control ($p < 0.01$), whereas reclustering was not significantly different from controls ($p > 0.1$). Data are from seven experiments and 179 synapses.

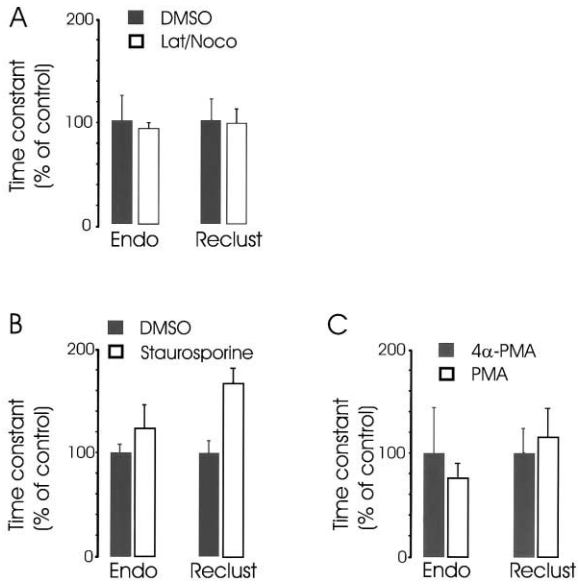

Figure 6. Reclustering Is Not Affected by Disruption of the Cytoskeleton but Is Slowed by the Kinase Inhibitor Staurosporine

(A) Treatment of cells with 20 μM latrunculin A and 10 μM nocodazole did not alter the time course of endocytosis or reclustering when compared to cells treated with only the vehicle (n = 5 experiments, 64 synapses).

(B) Treatment of cells with 2 μM staurosporine did not alter endocytic time course but significantly prolonged reclustering ($p < 0.005$; n = 5 experiments, 78 synapses). The average fractional change in fluorescence was lower for staurosporine-treated cells, indicating decreased total exocytosis of vesicles.

(C) Treatment of cells with 10 μM PMA did not alter time constant of endocytosis or reclustering when compared to treatment with the inactive form 4α-PMA ($p > 0.2$).

(line labeled "2"). Synapses adjacent to the bleached synapse lose an equivalent amount of fluorescence, suggesting that they are the source of the recovered fluorescence in the bleached synapse. A second argument that supports our idea that recovery requires lateral movement of fluorescent proteins from neighboring synapses is the following. In isolated synapses with the nearest vesicle cluster at least 10 μm away, recovery after photobleaching is very slow and is not accelerated by activity (Figure 7A, box labeled "4," Figure 7C, gray circle). Finally, in tetanus toxin-treated cells, there was little recovery of VAMP-EGFP in the bleached synapse, even after a 300 AP stimulus (Figure 7C, open circle).

Since increasing synaptic activity leads to greater surface dispersion of VAMP-EGFP, the degree of recovery of VAMP-EGFP fluorescence should depend on activity. We tested this by comparing the recovery obtained following 100 action potentials with that following 300 action potentials. Figure 7C shows the summary data from several experiments confirming our expectation.

It might seem surprising that the fluorescence at the bleached synapse recovers to nearly 60% of its prebleach value. This can be understood by realizing that the amount of recovery of fluorescence does not directly reflect the number of new VAMP-EGFP molecules incorporated into vesicles. This is because the fluorescence over the synapse is the sum of surface and internal fluorescence, and the fluorescence per EGFP in vesicles is three times lower than its fluorescence in the plasma membrane. Therefore, at rest, about 35% of the fluorescence is due to surface VAMP-EGFP. Correcting for this, the 58% recovery observed following 300 action potentials (Figure 7C) implies that about 30% of VAMP-EGFP in the synaptic vesicles of the bleached synapse is now from its neighboring synapses (Appendix). Another way to understand this is to note that, even in the absence of stimulation, about 28% of fluorescence is recovered at bleached synapses—this presumably corresponds to surface VAMP-EGFP. So, the extra fluorescence recovered after stimulation is ~30%, which would be vesicular VAMP-EGFP.

Discussion

The rapid increase in the information about the identity of molecular components involved in synaptic vesicle recycling has catalyzed physiological experiments aimed at understanding the mechanistic basis of this process. By perturbing different protein-protein interactions and observing their effects on synaptic physiology, potentially important late steps in release and early

Table 1. Protein Kinase Activity and Vesicle Trafficking Parameters

	$\Delta F/F$	$\tau_{endocytosis}$(s)	$\tau_{reclustering}$(s)
Control	0.30 ± 0.05	66.4 ± 12.1	134.2 ± 36.8
Staurosporine	0.21 ± 0.05 ($p < 0.01$)	81.7 ± 36.2 (NS)[a]	225.8 ± 44.6 ($p < 0.005$)
4α-PMA	0.30 ± 0.04 (NS)	77.9 ± 17.4 (NS)	134.6 ± 39.2 (NS)
PMA	0.27 ± 0.05 (NS)	61.0 ± 6.49 (NS)	155.3 ± 39.2 (NS)

[a] Not significantly different from control ($p > 0.01$).

steps in recovery have been identified (reviewed in Augustine et al., 1999; Brodin et al., 2000). Nevertheless, longstanding issues such as the mode, location, and time course of endocytosis at central synapses are incompletely understood. Even less well understood are the steps in postendocytic movement of vesicles at central synapses.

The classic ultrastructural studies in the neuromuscular junction indicated that clathrin-coated pits form at regions away from the active zone (Heuser and Reese, 1973; Miller and Heuser, 1984). More recent investigations on central synapses where endocytosis was perturbed have also found coated pits away from the active zone (Koenig and Ikeda, 1989; Takei et al., 1996; Shupliakov et al., 1997; Brodin et al., 2000). At the light microscopic level, immunofluorescence methods have been used to show that proteins involved in endocytosis are localized to regions surrounding the active zones of *Drosophila* neuromuscular junction (Roos and Kelly, 1999). This was taken to imply that vesicular components would be required to diffuse to these regions before endocytosis can occur. Recently, using FM1-43 and its congeners, Betz and colleagues demonstrated that two modes of endocytosis exist at the frog neuromuscular junction—one of them involving endocytosis at the peripheral regions (Richards et al., 2000). Another recent study using electron microscopy and low temperatures demonstrated that clathrin-mediated endocytosis also occurs close to the active zone (Teng and Wilkinson, 2000).

Although ultrastructural evidence has been presented to support peripheral endocytosis, real-time monitoring of this event has been elusive until now. Our experiments provide visual evidence for this process. Using a vesicular protein fused to different forms of GFP, we have tracked recycling events at small central synapses. Experiments with the strongly pH-sensitive ecl-spH revealed the time course of surface residence of the protein following exocytosis. On the other hand, VAMP-EGFP, which is less sensitive to pH changes between 5.5 and 7.4, allowed us to determine the location of the protein along the long axis of the synapse, whether located on the plasma membrane or on vesicles. Using the differential properties of the two probes, we inferred the time course of endocytosis and subsequent transport of vesicles to the synaptic cluster. Note that, although recent investigations using ecl-spH revealed the spreading of VAMP to perisynaptic regions, they could not dissociate reclustering and endocytosis (Sankaranarayanan and Ryan, 2000).

We find that ecl-spH, as suggested by recent studies (Miesenbock et al., 1998; Sankaranarayanan and Ryan, 2000), is a useful indicator of vesicle exocytosis and recapture. The signal-to-noise obtained from these probes allow detection of the exocytosis of as few as five vesicles at a synapse. Perhaps unexpectedly, we find that even VAMP-EGFP has enough signal-to-noise to allow detection of about 10 to 15 vesicles. More importantly, the lateral dispersion of VAMP-EGFP is a clear indicator of synaptic activity and may in fact be a useful indicator under conditions where resting ecl-spH fluorescence is too dim for detection (for example, in brain slices).

Even a relatively mild stimulus (40 action potentials) results in a slow recovery of spH fluorescence and detectable dispersion of VAMP-EGFP. This points to a complete fusion of vesicles with the plasma membrane, allowing protein components to escape to the plasma membrane. With this technique, it has not been possible so far to monitor single fusion events and the subsequent recovery. Therefore, we cannot be certain that a different mode of release, preventing the escape of vesicular components to the plasma membrane, exists under conditions of low-frequency stimulation. In fact, experiments using hypertonic stimulation have indicated that a fraction of vesicles can undergo kiss-and-run exocytosis (Pyle et al., 2000; Stevens and Williams, 2000). More recently, using the vacuolar ATPase inhibitor bafilomycin-A to trap vesicles in the alkaline state after exocytosis, Sankaranarayanan and Ryan demonstrated the absence of significant kiss-and-run exocytosis during action potential-evoked release (Sankaranarayanan and Ryan, 2001). Similarly, our results do not support purely kiss-and-run exocytosis, since we observed rapid dispersion of VAMP-EGFP even after mild stimulation.

The diffusion of VAMP along the plasma membrane following exocytosis may simply be a consequence of the mechanisms employed by synapses for recycling of vesicular components. If endocytosis occurs all along the presynaptic membrane and axon, after mild stimulation, the endocytic machinery near the active zone can operate quickly without allowing the vesicular components to diffuse away too far. With increasing stimulation, however, more vesicular components are inserted into the membrane. This might locally saturate the endocytic machinery (Sankaranarayanan and Ryan, 2000), and vesicular components can escape further away before they are all captured. The increased residence time might also reflect the time involved in separating *cis*-complexes of SNARE proteins (VAMP, syntaxin, and SNAP-25) by the action of N-ethylmaleimide-sensitive factor (NSF). This can be tested by perturbing the ATPase action of NSF using pharmacological or molecular methods.

We find that, like VAMP, synaptophysin is also inserted into the plasma membrane following exocytosis

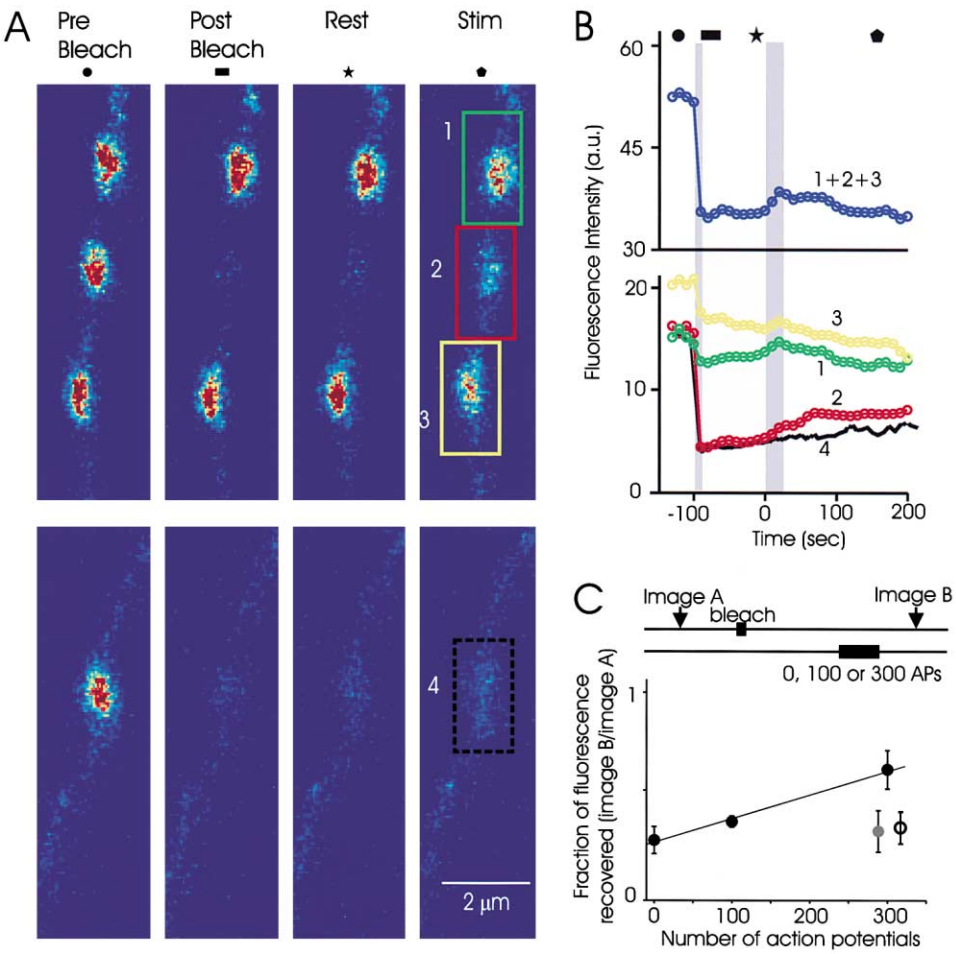

Figure 7. Spread of VAMP-EGFP to Neighboring Synapses

(A) Time-lapse images of a group of synapses expressing VAMP-EGFP. One of the synapses was bleached before acquiring the second image, which remained dim as along as no synaptic activity was evoked. Upon stimulation of action potentials, dispersion of fluorescence was observed at unbleached synapses, and the bleached synapse recovered some fluorescence (top sequence of images). If an isolated synapse was bleached, little fluorescence was recovered even after stimulation (bottom sequence of images). Symbols on top of images refer to corresponding time points indicated in Figure 7B.

(B) Fluorescence intensity measured in three regions encompassing individual synapses shows characteristic pattern. After bleaching, the middle synapse (labeled "2") loses most of its fluorescence, while the other two remain essentially unaltered. During stimulation (indicated by the width of the gray bar), the fluorescence in the middle synapse starts increasing and stays high, while the fluorescence in the neighboring synapses decrease (labels "1" and "3"). The summed fluorescence intensity of the three synapses ("1+2+3") increases upon stimulation and recovers to prestimulus level, indicating that there is no net change in VAMP-EGFP fluorescence. A different synapse (labeled "4") that was >10 μm away from a neighbor did not recover much fluorescence when bleached (dashed line).

(C) Fluorescence recovery as a function of the stimulus strength: 0, 100, or 300 action potentials at 10 Hz. The gray circle represents data from synapses that had no neighbors within 10 μm on either side. Recovery at these isolated synapses was not significantly different from the nonstimulated condition. At tetanus toxin-treated synapses (open circle), recovery was not significantly different from nonstimulated synapses. Error bars represent one standard deviation. n = 6 for each data point, except tetanus toxin experiment, where n = 4. The straight line is drawn only to draw attention to the trend in the activity-dependent recovery.

and diffuses to the axonal membrane. The kinetics of transport of recovered synaptophysin are similar to that of VAMP. This can be parsimoniously explained by assuming that both proteins are transported together in the same set of vesicles. This is especially likely if synaptic vesicles are directly made at the plasma membrane, without the need for further sorting (Takei et al., 1996; Murthy and Stevens, 1998). Future experiments using spectrally separated variants of GFP can help determine the extent to which different vesicle proteins remain together during various legs of the synaptic vesicle cycle.

What are the mechanisms in translocation of newly endocytosed vesicles to the synaptic vesicle clusters? Since newly endocytosed vesicles are not randomly distributed along the axon, the mechanism is either active or, if passive, involves some sort of rectified Brownian motion. We tested the hypothesis that cytoskeletal elements such as actin filaments or microtubules are involved and found little evidence to support it. Neither latrunculin nor nocodazole was able to alter the magnitude or time course of endocytosis and reclustering. Although we obtained evidence for the disruption of dynamic actin by latrunculin (disruption of stress fibers

in astrocytes, loss of actin from dendritic spines), we could not be sure that actin in the presynaptic terminal was disrupted. Since it was difficult to observe robust staining of actin (with phalloidin or actin-GFP) in presynaptic terminals in our mass cultures, we were not able to look for disruption of this staining after latrunculin treatment. Therefore, it remains possible that a small but essential pool of filamentous actin remains resistant to our treatment and participates in reclustering. A recent study indicated that disruption of actin using latrunculin A causes an increase in release probability but no alteration in the rate of refilling of the readily releasable pool (Morales et al., 2000).

We found that the kinase inhibitor staurosporine slows down reclustering. Although the exact target of staurosporine is unclear at present, PKC is a likely candidate, since its activation is thought to speed up refilling of the readily releasable pool (Stevens and Sullivan, 1998). If inhibition of PKC is responsible for slowing down reclustering, activation of this kinase may have the opposite effect. Our experiments did not support this expectation. It may be because stimulation with 300 APs may maximally activate PKC and addition of phorbol esters may not have additional effect. Monitoring reclustering after weak stimuli might reveal a role for PKC. We are currently testing whether other kinases play a role in reclustering. One potential candidate is myosin light chain kinase, since it is thought to play a role in mobilization of vesicles at hippocampal synapses (Ryan, 1999). Interestingly, staurosporine is also thought to inhibit vesicle mobilization at some synapses (Kraszewski et al., 1996; Becherer et al., 2001). A distinction must be made, however, between vesicle mobilization studied by those authors and reclustering investigated here. Previous experiments were directed at movement of vesicles from the reserve pool to the releasable pool (Kraszewski et al., 1996; Becherer et al., 2001). Our experiments address a different leg of the vesicle's journey—that from endocytic sites to the reserve vesicle cluster. One could not have been sure, a priori, that the two different steps in vesicle movement share common mechanisms; we have provided experimental support for it.

Based on our findings and other published results, we propose the following model for reclustering. At rest vesicles are clustered due to some attractive interaction between them, for example, due to vesicle-associated proteins such as synapsins (Greengard et al., 1993; Hosaka et al., 1999). Activity "loosens" the vesicles by decreasing their attractive interaction—this can be due to dissociation of synapsins from vesicles in a phosphorylation-dependent manner (Torri-Tarelli et al., 1992; Hosaka et al., 1999). When activity subsides, vesicles are reformed at various locations at the synapse. If proteins such as synapsins are now dispersed along the axon, they will be able to reattach themselves to the newly endocytosed vesicle and confer stickiness to it. Even if the newly formed vesicle makes random Brownian movements along the axon, it will soon encounter the nearest vesicle cluster and get stuck there. When kinase activity is blocked, vesicles are not loosened, and synapsins do not dissociate from the vesicles. Newly endocytosed vesicles will not have free synapsins to confer stickiness to them, and they will take longer to find the synaptic vesicle cluster.

Previous experiments have indicated that, following endocytosis, the vesicle can remain largely intact, without mixing with intermediate compartments during recycling (Murthy and Stevens, 1998). This, however, does not imply preservation of vesicular components in the step(s) between exocytosis and endocytosis. In fact, the present study indicates that vesicular proteins such as VAMP diffuse relatively quickly along the plasma membrane, and endocytosis will reclaim proteins that originally belonged to different vesicles. In fact, mixing of vesicular components can occur even across neighboring synapses (Figure 7). The critical issue, however, is whether the process of endocytosis is efficient in selectively recruiting the appropriate vesicular proteins for each new vesicle formed. If this is so, then there is no logical requirement for further sorting. Similar rates of reclustering observed for VAMP and synaptophysin argue for common vesicular carriers, which will also obviate a need for sorting.

The observation that a vesicle protein can move from one synapse to a neighboring one following sustained activity raises interesting questions regarding the independence of adjacent synapses (Engert and Bonhoeffer, 1997; Murthy, 1997). The efficacy of presynaptic function is presumably determined by vesicle pool sizes and how release is drawn from them. These physical parameters will be dictated in turn by the molecular state of the components, such as the extent of phosphorylation or isoform identity. If these molecules are able to move between synapses, they might carry information regarding the strength of a synapse from one synapse to the next resulting in "cross-talk." This will occur to a greater extent during strong activity (of the sort used during induction of long-term potentiation), during which the protein can diffuse significant distances between adjacent boutons. Our experiments, therefore, reveal a hitherto unsuspected phenomenon that might contribute to the correlation between properties of adjacent synapses (Murthy et al., 1997).

Our experiments also illustrate the manner in which trafficking of vesicles and their components can be monitored even at small central synapses, using molecular markers. Spectrally separated variants of GFP and other proteins can be fused to different synaptic proteins and simultaneously monitored to determine their progress through the synaptic vesicle cycle. Additionally, these fusion proteins can also be used to track changes in morphology and composition of synapses during development or plasticity.

In summary, we have confirmed previous reports indicating that evoked exocytosis at small central synapses generally involves full fusion of vesicular membrane with no barrier for lateral diffusion of vesicular proteins. Endocytosis following fusion occurs at the peripheral regions surrounding the active zone. An additional step in vesicle trafficking involving the transport of endocytosed vesicles to the main vesicle cluster was directly visualized. Increasing activity slows the rate of endocytosis as well as reclustering. We could not find evidence for the role of actin filaments and microtubules in reclustering. Protein kinases, however, appear to regulate the rate of reclustering.

Experimental Procedures

Cultures and Transfection

Hippocampal neurons were dissociated from 1- to 3-day-old rats, using methods described previously (Murthy et al., 1997). VAMP2-EGFP construct was a gift from Richard Scheller. Ecliptic synaptopHluorin (Miesenbock et al., 1998) and superecliptic synaptopHluorin (with substitutions F64L and S65T) were gifts from James Rothman. These two proteins have GFP fused to the lumenal C terminus of VAMP. Synaptophysin-EGFP (EGFP fused to the C terminus of synaptophysin) was a gift of Jane Sullivan. Neurons were typically transfected at 6–7 days in vitro using the calcium phosphate method (Xia et al., 1996). Transfected cultures were allowed to grow for another week, allowing mature synapses to develop. Experiments were done when cells were 13–15 days in vitro and at room temperature (20°C–22°C).

Treatment with Pharmacological Agents

Several experiments involved treatment with pharmacological agents; we describe them here. NH_4Cl was prepared by replacing 50 mM NaCl and buffered to pH 7.4. For experiments using exogenous calcium buffers, we incubated neurons in 100 μM EGTA-AM (0.02% DMSO, 0.005% pluronic F127) for 10 min followed by a 3 min wash in control medium. Incubation was done in the recording chamber on the microscope stage, and experiments were done immediately afterwards. A similar protocol was used for treatment with a mixture of 20 μM latrunculin A and 10 μM nocodazole (0.4% DMSO). Incubation times were 15 min, by which time clear morphological changes were observed. Longer incubation times were also used, but they led to a gross disruption of the cultures. Since the results were not different for longer incubation times, we preferred the shorter times. For experiments with staurosporine, cultures were incubated for 1 hr in 2 μM staurosporine in 0.04% DMSO in the culture incubator at 37°C. Treated and control cells (treated with just DMSO) from neighboring wells were then mounted on the recording chambers for experimentation. Active and inactive phorbol esters (phorbol 12-myristate 13-acetate and 4α-phorbol 12-myristate 13-acetate, respectively) were added to the cells while they were mounted on the microscope chamber at a concentration of 10 μM in 0.1% DMSO. Tetanus toxin was reconstituted in distilled water to a final concentration of 10 nM, and cells were incubated in toxin-containing medium for 16 hr in the incubator. Compounds were obtained from the following sources: EGTA-AM, Molecular Probes, Eugene, OR; latrunculin A, nocodazole, staurosporine, PMA, and 4α-PMA, RBI; tetanus toxin, List Laboratories.

Imaging

For the imaging experiments, a closed, small volume, laminar flow chamber (Warner Instruments) was mounted on a movable stage of a microscope. The chamber incorporates two coverslips, the bottom one containing cells, and a pair of platinum wires separated by about 5 mm for field stimulation. The 25 mm coverslip with cells formed the bottom of the chamber, and neurons could be viewed with an oil lens (60×, 1.35 NA, Olympus) of the inverted microscope. All experiments were done in HEPES-buffered saline (136 mM NaCl, 2.5 mM KCl, 10 mM HEPES, 10 mM D-glucose, 2 mM $CaCl_2$, 1.3 mM $MgCl_2$) containing 50 μM APV and 10 μM CNQX to block recurrent activity. A Grass SD9 stimulator was used to evoke action potentials, using brief voltage pulses (1 ms, 20V–50V, bipolar) applied to the platinum wires.

Synaptic vesicles were labeled with the styryl dye FM4-64 (Molecular Probes) by bathing the cultures in HBS containing 5–10 μM dye and eliciting 300 action potentials at 10 Hz. After stimulation, neurons were bathed in the dye-containing medium for another minute to allow for complete recapture of exocytosed vesicular membrane. Cells were then perfused with dye-free HBS for 10 min to remove surface dye. After obtaining images of labeled synapses, neurons were stimulated again to evoke exocytosis and release of FM4-64 from vesicles, which is visualized as a loss of fluorescence.

Images were acquried using a cooled CCD camera (PCO Sensicam, Cooke Corporation) on an Olympus inverted microscope (IX-70) with a 60×, 1.35 NA oil lens. Light from a mercury lamp was shuttered using a Uniblitz shutter (Vincent Associates). All three VAMP fusion proteins were excited using 470–490 nm, and the emitted light was collected through a 505–550 nm band-pass filter. For FM4-64 imaging, excitation was at 530 ± 20 nm, and emitted light was collected using a 590 nm long-pass filter. Images were typically collected using the entire chip (1280 × 1024 pixels, 0.11 μm pixel size in the images) and stored for offline analysis. The photobleaching experiments with VAMP-EGFP were done using a confocal microscope (Fluoview, Olympus) attached to a BX50-WI upright microscope, using a 40×, 0.8NA water immersion lens. The 488 nm line of an Argon laser was used for excitation, and the emitted light was filtered with a 505–550 band-pass filter. The pinhole was set to be around 5 Airy disks in diameter to obtain a bigger depth of field.

Data Analysis

Images were analyzed using custom-written routines in MATLAB (MathWorks Inc., Natick, MA). Regions of interest (ROI) were drawn around synaptic boutons, and the average intensity was calculated. For each synapse, the center of intensity was calculated to correct for any image shifts over the course of the experiment. Fluorescence is expressed in intensity units that correspond to fluorescence values averaged over all pixels within the region of interest. For analysis of dispersion and reclustering, boxes were chosen in the periphery of synapses, about 1 μm from the center of intensity of the synapse. FM4-64 analysis was identical to previously published work (Murthy and Stevens, 1998). The decay of fluorescence was fitted with a single exponential. In some experiments, fluorescence decay deviated from monoexponential behavior. In these cases, we obtained the best-fitting single exponential function from the early portion of decay. We also occasionally encountered a delay in the decay of fluorescence following termination of stimulation; we then fitted the exponential function after excluding the early delay. Data are presented as mean ± SEM, except when noted otherwise.

Appendix

Measuring Exocytosis with VAMP-EGFP

If EGFP was pH insensitive, exocytosis would not lead to any change in VAMP-EGFP fluorescence. Since EGFP fluorescence does change 3-fold when going from vesicular pH of about 5.5 to the extracellular pH of about 7.4 (Kneen et al., 1998; Llopis et al., 1998), we can use it to detect exocytosis. Here, we relate the fractional change in fluorescence of VAMP-EGFP upon exocytosis to the fraction of vesicles released.

Let T be the total number of vesicles, f the fluorescence of a single vesicle at neutral pH, q the quenching by intravesicular pH, and r the number of vesicles released.

The total fluorescence in a bouton at rest is the sum of the vesicular and surface VAMP-EGFP (F_v and F_s, respectively):

$$F_T = F_v + F_s$$

The vesicular fluorescence is

$$F_v = Tfq$$

Since about 15% of the total VAMP-EGFP is resident on the surface (Sankaranarayanan and Ryan, 2000), we can estimate its fluorescence F_s from the relation

$$0.15 = \frac{F_s}{Tf + F_s}$$

This leads to the relation

$$F_s = 0.176Tf$$

Therefore,

$$F_T = Tqf + 0.176Tf$$

Following stimulation (before significant endocytosis has occurred), the fluorescence is

$$F_{stim} = (T - r)qf + rf + 0.176Tf$$

The change in fluorescence is

$$\Delta F_{stim} = (F_{stim} - F_T) = rf(1 - q) = 0.67rf$$

since $q = 0.33$.

The fractional change in fluorescence is given by

$$\frac{\Delta F_{stim}}{F_T} = \frac{rf(1 - q)}{(Tqf + 0.176Tf)} = \frac{0.67rf}{0.51Tf} = 1.31\left(\frac{r}{T}\right)$$

Since r/T is the fractional exocytosis, we see that measuring $\Delta F/F$ allows us to estimate the fractional release. This calculation is valid for short stimuli when significant endocytosis has not occurred. Using published data (Sankaranarayanan and Ryan, 2001), we estimate that for a 40 AP stimulus at 10 Hz, less than 10% endocytosis would have occurred in the 2 s period.

A Simple Model for Reclustering of VAMP

We assume that, following exocytosis, there are two pools of VAMP-EGFP in the peripheral regions: exposed and internalized VAMP-EGFP. There are two processes that cause reduction of the fluorescence in the periphery: endocytosis (and immediate acidification) and movement of internalized VAMP-EGFP to the center of the synapse. If each of these processes is considered to occur nearly irreversibly on the time scale and conditions of our experiments, the reaction is given by

$$Vpe \xrightarrow{k_1} Vpi \xrightarrow{k_2} Vci$$

where *Vpe* is the exposed VAMP in periphery, *Vpi* is the internalized VAMP in the periphery, and *Vci* is the internalized VAMP in the central region of the synapse. The set of differential equations governing the movement can be solved explicitly and the expressions for *Vpe* and *Vpi* obtained.

$$V_{pe} = Ae^{-k_1 t}$$

$$V_{pi} = A\frac{k_1}{k_1 - k_2}(e^{-k_1 t} - e^{-k_2 t})$$

Were there no quenching of VAMP-EGFP upon internalization, the total fluorescence in the periphery will be proportional to (*Vpe* + *Vpi*). Since internalized VAMP-EGFP is quenched 3-fold, the actual fluorescence measured will be (*Vpe* + 0.33 × *Vpi*). The difference in the time course of decay of the two expressions is illustrated in Figure 3A.

Quantifying VAMP-EGFP Recovery after Photobleaching

In experiments on mixing of VAMP-EGFP between neighboring synapses, the measured quantity is fluorescence intensity. This does not directly correspond to the number of vesicles, because of the unequal contribution of surface and vesicular VAMP-EGFP to fluorescence emission (because of the pH dependence). Here, we derive the correction factor to convert fluorescence intensities into fraction of VAMP-EGFP molecules.

We use a similar notation as above, except for two new superscripts: F^o refers to quantities before bleaching and F^b after bleaching. Before bleaching, the fluorescence intensity at a synapse is given by

$$F_T^o = F_v^o + F_s^o$$

$$F_T^o = Tqf + 0.176Tf = 0.506Tf$$

$$\frac{F_s^o}{F_T^o} = \frac{0.176Tf}{0.506Tf} = 0.35$$

$$\frac{F_v^o}{F_T^o} = \frac{0.33Tf}{0.506Tf} = 0.65$$

After bleaching and subsequent stimulation with 300 APs, the fluorescence at the bleached synapse was experimentally determined to be

$$F_T^b = 0.55F_T^o = F_v^b + F_s^b$$

If we assume that surface fluorescence recovers completely (a conservative estimate as we will see below),

$$F_s^b = F_s^o = 0.35F_T^o$$

$$F_v^b = 0.55F_T^o - 0.35F_T^o = 0.2F_T^o = 0.31F_v^o$$

Therefore, about 30% of the vesicular VAMP is from neighboring synapses. If surface fluorescence has not fully recovered following stimulation, then the proportion of VAMP from neighboring synapses will be even larger.

Acknowledgments

We thank Richard Scheller for VAMP-EGFP; James Rothman, Gero Miesebock, and Dino de Angelis for the pHluorins; and Jane Sullivan for synaptophysin-EGFP. We are grateful to Erin Star for her assistance in the experiments testing the role of cytoskeleton in reclustering. We thank Juan Burrone for fruitful interactions over the course of the study. The study was supported by startup funds from Harvard University and a grant from the National Institutes of Health. V.N.M. is a Pew Scholar and an Alfred P. Sloan Foundation Fellow.

Received October 20, 2000; revised June 7, 2001.

References

Ahmari, S.E., Buchanan, J., and Smith, S.J. (2000). Assembly of presynaptic active zones from cytoplasmic transport packets. Nat. Neurosci. *3*, 445–451.

Augustine, G.J., Burns, M.E., DeBello, W.M., Hilfiker, S., Morgan, J.R., Schweizer, F.E., Tokumaru, H., and Umayahara, K. (1999). Proteins involved in synaptic vesicle trafficking. J. Physiol. *520*, 33–41.

Becherer, U., Guatimosim, C., and Betz, W.J. (2001). Effects of staurosporine on exocytosis and endocytosis at frog motor nerve terminals. J. Neurosci. *21*, 782–787.

Bellen, H. (1999). Neurotransmitter Release, Volume *23*, B.D. Hames and D. M. Glover, eds. (Oxford: Oxford University Press).

Brodin, L., Low, P., and Shupliakov, O. (2000). Sequential steps in clathrin-mediated synaptic vesicle endocytosis. Curr. Opin. Neurobiol. *10*, 312–320.

Calakos, N., and Scheller, R.H. (1996). Synaptic vesicle biogenesis, docking and fusion: a molecular description. Physiol. Rev. *76*, 1–29.

Ceccarelli, B., Hurlbut, W.P., and Mauro, A. (1973). Turnover of transmitter and synaptic vesicles at the frog neuromuscular junction. J. Cell Biol. *57*, 499–524.

Cummings, D.D., Wilcox, K.S., and Dichter, M.A. (1996). Calcium-dependent paired-pulse facilitation of miniature EPSC frequency accompanies depression of EPSCs at hippocampal synapses in culture. J. Neurosci. *16*, 5312–5323.

Dobrunz, L.E., and Stevens, C.F. (1997). Heterogeneity of release probability, facilitation, and depletion at central synapses. Neuron *18*, 995–1008.

Dreyer, F., Mallart, A., and Brigant, J.L. (1983). Botulinum A toxin and tetanus toxin do not affect presynaptic membrane currents in mammalian motor nerve endings. Brain Res. *270*, 373–375.

Engert, F., and Bonhoeffer, T. (1997). Synapse specificity of long-term potentiation breaks down at short distances. Nature *388*, 279–284.

Fesce, R., Grohovaz, F., Valtorta, F., and Meldolesi, J. (1994). Neurotransmitter release: fusion or 'kiss-and-run'? Trends Cell Biol. *4*, 1–4.

Gad, H., Low, P., Zotova, E., Brodin, L., and Shupliakov, O. (1998). Dissociation between Ca2+-triggered synaptic vesicle exocytosis and clathrin-mediated endocytosis at a central synapse. Neuron *21*, 607–616.

Greengard, P., Valtorta, F., Czernik, A.J., and Benfenati, F. (1993). Synaptic vesicle phosphoproteins and regulation of synaptic function. Science *259*, 780–785.

Han, W., Li, D., Stout, A.K., Takimoto, K., and Levitan, E.S. (1999). Ca2+-induced deprotonation of peptide hormones inside secretory vesicles in preparation for release. J. Neurosci. *19*, 900–905.

Heuser, J.E., and Reese, T.S. (1973). Evidence for recycling of synaptic vesicle membrane during transmitter release at the frog neuromuscular junction. J. Cell Biol. *57*, 315–344.

Hosaka, M., Hammer, R.E., and Sudhof, T.C. (1999). A phospho-

switch controls the dynamic association of synapsins with synaptic vesicles. Neuron *24*, 377–387.

Katz, B. (1969). The Release of Neural Transmitter Substances (Liverpool: Liverpool University Press).

Klingauf, J., Kavalali, E.T., and Tsien, R.W. (1998). Kinetics and regulation of fast endocytosis at hippocampal synapses. Nature *394*, 581–585.

Kneen, M., Farinas, J., Li, Y., and Verkman, A.S. (1998). Green fluorescent protein as a noninvasive intracellular pH indicator. Biophys. J. *74*, 1591–1598.

Koenig, J.H., and Ikeda, K. (1989). Disappearance and reformation of synaptic vesicle membrane upon transmitter release observed under reversible blockage of membrane retrieval. J. Neurosci. *9*, 3844–3860.

Kraszewski, K., Daniell, L., Mundigl, O., and de Camilli, P. (1996). Mobility of synaptic vesicles in nerve endings monitored by recovery from photobleaching of synaptic vesicle-associated fluorescence. J. Neurosci. *16*, 5905–5913.

Llopis, J., McCaffery, J.M., Miyawaki, A., Farquhar, M.G., and Tsien, R.Y. (1998). Measurement of cytosolic, mitochondrial, and Golgi pH in single living cells with green fluorescent proteins. Proc. Natl. Acad. Sci. USA *95*, 6803–6808.

Miesenbock, G., De Angelis, D.A., and Rothman, J.E. (1998). Visualizing secretion and synaptic transmission with pH-sensitive green fluorescence proteins. Nature *394*, 192–195.

Miller, T.M., and Heuser, J.E. (1984). Endocytosis of synaptic vesicle membrane at the frog neuromuscular junction. J. Cell Biol. *98*, 685–698.

Morales, M., Colicos, M.A., and Goda, Y. (2000). Actin-dependent regulation of neurotransmitter release at central synapses. Neuron *27*, 539–550.

Murthy, V.N. (1997). Synaptic plasticity: neighborhood influences. Curr. Biol. *7*, R512–R515.

Murthy, V.N. (1999). Optical detection of synaptic vesicle exocytosis and endocytosis. Curr. Opin. Neurobiol. *9*, 314–320.

Murthy, V.N., and Stevens, C.F. (1998). Synaptic vesicles retain their identity through the endocytic cycle. Nature *392*, 497–501.

Murthy, V.N., Sejnowski, T.J., and Stevens, C.F. (1997). Heterogeneous release properties of visualized individual hippocampal synapses. Neuron *18*, 599–612.

Neale, E.A., Bowers, L.M., Jia, M., Bateman, K.E., and Williamson, L.C. (1999). Botulinum neurotoxin A blocks synaptic vesicle exocytosis but not endocytosis at the nerve terminal. J. Cell Biol. *147*, 1249–1260.

Parfitt, K.D., and Madison, D.V. (1993). Phorbol esters enhance synaptic transmission by a presynaptic calcium-dependent mechanism in rat hippocampus. J. Physiol. *471*, 245–268.

Prekeris, R., and Terrian, D. (1997). Brain myosin V is a synaptic vesicle-associated motor protein: evidence for a Ca2+-dependent interaction with the synaptobrevin-synaptophysin complex. J. Cell Biol. *137*, 1589–1601.

Pyle, J.L., Kavalali, E.T., Piedras-Renteria, E.S., and Tsien, R.W. (2000). Rapid reuse of readily releasable pool vesicles at hippocampal synapses. Neuron *28*, 221–231.

Richards, D.A., Guatimosim, C., and Betz, W.J. (2000). Two endocytic recycling routes fill two vesicle pools in frog motor nerve terminals. Neuron *27*, 551–559.

Roos, J., and Kelly, R.B. (1999). The endocytic machinery in nerve terminals surrounds sites of exocytosis. Curr. Biol. *9*, 1411–1414.

Ryan, T.A. (1999). Inhibitors of myosin light chain kinase block synaptic vesicle pool mobilization during action potential firing. J. Neurosci. *19*, 1317–1323.

Ryan, T.A., Smith, S.J., and Reuter, H. (1996). The timing of synaptic vesicle endocytosis. Proc. Natl. Acad. Sci. USA *93*, 5567–5571.

Sankaranarayanan, S., and Ryan, T.A. (2000). Real-time measurements of vesicle-SNARE recycling in synapses of the central nervous system. Nat. Cell Biol. *2*, 197–204.

Sankaranarayanan, S., and Ryan, T.A. (2001). Calcium accelerates endocytosis of vSNAREs at hippocampal synapses. Nat. Neurosci. *4*, 129–136.

Schiavo, G., Benfenati, F., Poulain, B., Rossetto, O., Polverino de Laureto, P., DasGupta, B.R., and Montecucco, C. (1992). Tetanus and botulinum-B neurotoxins block neurotransmitter release by proteolytic cleavage of synaptobrevin. Nature *359*, 832–835.

Schikorski, T., and Stevens, C.F. (1997). Quantitative ultrastructural analysis of hippocampal excitatory synapses. J. Neurosci. *17*, 5858–5867.

Shupliakov, O., Low, P., Grabs, D., Gad, H., Chen, O., David, C., Takei, K., de Camilli, P., and Brodin, L. (1997). Synaptic vesicle endocytosis impaired by disruption of dynamin-SH3 domain interactions. Science *276*, 259–263.

Stevens, C.F., and Sullivan, J.M. (1998). Regulation of the readily releasable vesicle pool by protein kinase C. Neuron *21*, 885–893.

Stevens, C.F., and Williams, J. (2000). A novel mode of exocytosis at hippocampal synapses. Proc. Natl. Acad. Sci. USA, *97*, 12828–12833.

Südhof, T.C. (1995). The synaptic vesicle cycle: a cascade of protein-protein interactions. Nature *375*, 645–653.

Takei, K., Mundigl, O., Daniell, L., and de Camilli, P. (1996). The synaptic vesicle cycle: a single vesicle budding step involving clathrin and dynamin. J. Cell Biol. *133*, 1237–1250.

Teng, H., and Wilkinson, R.S. (2000). Clathrin-mediated endocytosis near active zones in snake motor boutons. J. Neurosci. *20*, 7986–7993.

Torri-Tarelli, F., Bossi, M., Fesce, R., Greengard, P., and Valtorta, F. (1992). Synapsin I partially dissociates from synaptic vesicles during exocytosis induced by electrical stimulation. Neuron *9*, 1143–1153.

von Gersdorff, H., and Matthews, G. (1994). Dynamics of synaptic vesicle fusion and membrane retrieval in synaptic terminals. Nature *367*, 735–739.

Waters, J., and Smith, S.J. (2000). Phorbol esters potentiate evoked and spontaneous release by different presynaptic mechanisms. J. Neurosci. *20*, 7863–7870.

Xia, Z., Dudek, H., Miranti, C.K., and Greenberg, M.E. (1996). Calcium influx via the NMDA receptor induces immediate early gene transcription by a MAP kinase/ERK-dependent mechanism. J. Neurosci. *16*, 5425–5436.

Yonekawa, Y., Harada, A., Okada, Y., Funakoshi, T., Kanai, Y., Takei, Y., Terada, S., Noda, T., and Hirokawa, N. (1998). Defect in synaptic vesicle precursor transport and neuronal cell death in KIF1A motor protein-deficient mice. J. Cell Biol. *141*, 431–441.

Zenisek, D., Steyer, J.A., and Almers, W. (2000). Transport, capture and exocytosis of single synaptic vesicles at active zones. Nature *406*, 849–854.